Deformation of the 2002 Denali Fault Earthquakes, Mapped by Radarsat-1 Interferometry

PAGES 425, 430–431

The magnitude 7.9 earthquake that struck central Alaska on 3 November 2002 was the largest strike-slip earthquake in North America for more than 150 years. The earthquake ruptured about 340 km of the Denali Fault system with observed right-lateral offsets of up to 9 m [*Eberhart-Phillips et al.*, 2003] (Figure 1). The rupture initiated with slip on a previously unknown thrust fault, the 40-km-long Susitna Glacier Fault. The rupture propagated eastward for about 220 km along the right-lateral Denali Fault where right-lateral slip averaged ~5 m, before stepping southeastward onto the Totschunda Fault for about 70 km, with offsets as large as 2 m. The 3 November earthquake was preceded by a magnitude 6.7 shock on 23 October—the Nenana Mountain Earthquake—which was located about 25 km to the west of the 3 November earthquake.

This article discusses the mapping of the co-seismic displacements associated with the 23 October 2002 Nenana Mountain earthquake and the 3 November 2002 Denali earthquake by satellite radar imagery.

Displacement Mapped with Radarsat-1 Interferograms

The interferometric synthetic aperture radar (InSAR) technique was used to map the co-seismic displacements that resulted from the 23 October and 3 November earthquakes, with synthetic aperture radar (SAR) images collected by the Radarsat-1 satellite. InSAR utilizes two or more SAR images of the same area acquired at different times to map ground deformation at a horizontal resolution of tens of meters over large areas with centimeter to sub-centimeter precision [e.g., *Massonnet and Feigl*, 1998]. Interferograms are only sensitive to the component of surface deformation toward or away from the satellite, in their line of sight. The preliminary analysis of interferograms over the Denali Fault zone suggested that C-band (wavelength of 5.66 cm) ERS and Radarsat-1 interferograms can maintain coherence up to 2–3 years over the valleys and low-relief areas that are not densely forested [*Ford et al.*, 2002; *Wright et al.*, 2002]. However, coherence is lost over glacier-blanketed areas along the Denali Fault and other severely rugged terrains. In this article, the two-pass InSAR method [*Massonnet and Feigl*, 1998] with the U.S. Geological Survey (USGS) 15-minute Alaska DEM was used to correct for the topographic contribution to the observed phase values. The DEM has a specified horizontal accuracy of ~60 m and root-mean-square vertical error of ~15 m, resulting in no more than ~5 mm of line-of-sight error in our interferograms [e.g., *Massonnet and Feigl*, 1998]. The interferograms were acquired on a mixture of ascending and descending passes, covering intervals of 24 to 96 days.

The interferogram from two SAR images acquired during ascending satellite passes, where Radarsat-1 traveled from south to north and looked to the east (Figure 1, Table 1), shows that the northern block of the Denali Fault moved away from the satellite with respect to the southern block, corresponding to the right-lateral movement associated with the 3 November rupture. Also, the thrusting movement over the Susitna Glacier Fault is obvious; the northwestern block moved upward toward the satellite. The right-lateral movement of the 3 November event is also apparent in the interferogram from two descending-pass SAR images when Radarsat-1 traveled from north to south and looked to the west (Figure 2a, Table 1). However, the movement associated with the Susitna Fault is not observable. Subsidence south of the Susitna Fault, and uplift north of it, cannot be seen because they cause phase changes with the same sign as the right-lateral motion on the main Denali Fault.

Due to the difference in imaging geometry, fringe patterns near the Susitna Fault appear different in the ascending and descending interferograms (Figures 1 and 2a). Because an interferogram can only map the ground surface deformation along the satellite look direction, it is ambiguous to infer the 3-D deformation of ground targets from a single interferogram. Using interferograms from ascending and descending passes makes it possible to better determine the orientation of the Susitna Glacier Fault and the direction of the slip vector on it.

Another ascending interferogram maps more than 95 cm of right-lateral displacement associated with the 3 November earthquake (Figure 2b, Table 1). The interferometric coherence is excellent over areas along the trans-Alaska oil pipeline (Figures 1 and 2b). Assuming the northern block of the Denali Fault moved toward E15°S, this amount of line-of-sight displacement corresponds to about 140 cm

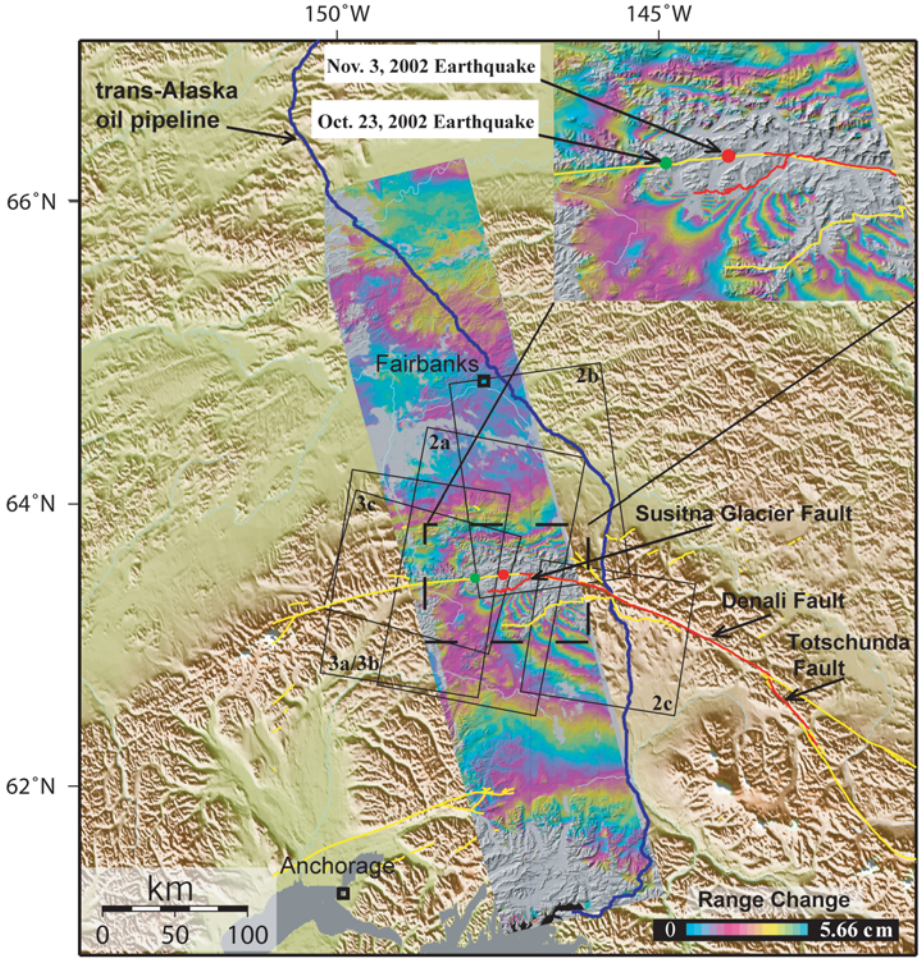

Fig. 1. Radarsat-1 interferogram showing the displacement over the western part of the 340-km-long surface ruptures (red lines) associated with the M 7.9 3 November 2002 Denali earthquake (Table 1). The yellow lines represent faults that show evidence of activity during Quaternary time. The polygons represent locations of figures shown in Figures 2 and 3. A zoomed portion of the interferogram with dense fringes outlined by the dashed box is shown in the upper right corner. The interferogram is draped over the shaded relief images, and areas without interferometric coherence are uncolored.

By Zhong Lu, Tim Wright, and Chuck Wicks

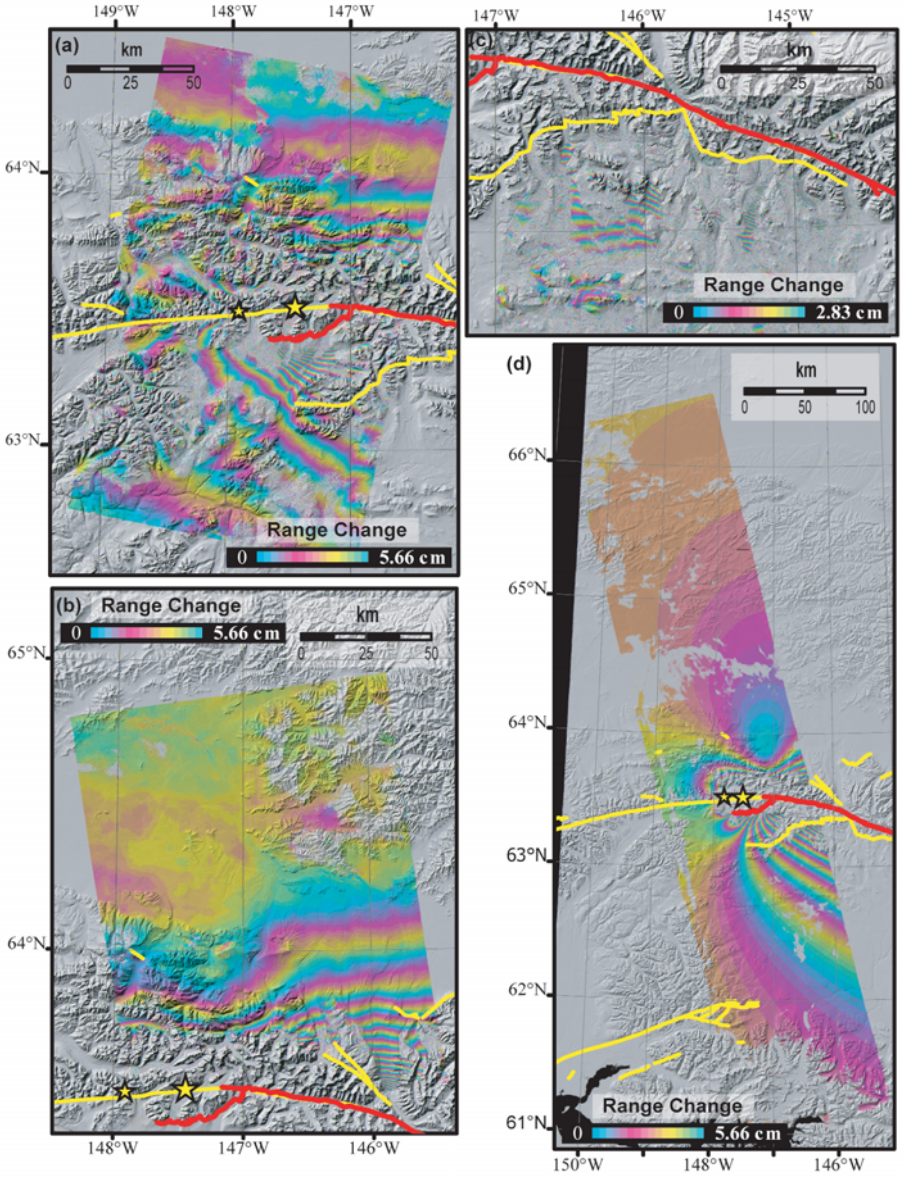

Fig. 2. (a-c) Radarsat-1 interferograms showing the displacement over the western part of the ruptures associated with the 3 November 2002 Denali earthquake. SAR image acquisition times are shown in Table 1. (d) A synthetic interferogram using parameters that best fit the observed interferograms. The epicenters of the 3 November event (the larger star) and the 23 October 2002 shock (the smaller star) are also shown.

right-lateral movement on the northern block of the Denali Fault. Assuming that the deformation is symmetrical across the fault, more than 280-cm right-lateral movement can be inferred from this interferogram. This is likely to be an underestimate, as we do not have data right up to the fault. Unfortunately, no data were collected to the south of the Denali Fault on these satellite passes.

The only interferogram processed that covers the central part of the rupture has the poorest coherence (Figure 2c, Table 1). Fringes are visible over several valleys and sparsely vegetated areas. The poor coherence is also due to the baseline for this interferogram, about 200 m, which is the largest of all the interferograms.

Three interferograms were used to map the deformation associated with the 23 October Nenana Mountain earthquake (Figures 3a-3c, Table 1). These images show the right-lateral movement associated with the 23 October shock.

Table 1. SAR Images Used For This Study.

Date 1	*Date 2*	*Incidence angle (°)*	*Track angle (°)*	*B_{perp} (m)*	*Figure*
20021029	20021122	27.7	-14.5	110	Fig. 1
20021020	20021113	39.5	-169.1	-10	Fig. 2a
20021011	20021104	47.0	-8.1	158	Fig. 2b
20020813	20021117	44.4	-170.9	197	Fig. 2c
20020816	20021027	44.4	-170.9	-16	Fig. 3a
20021003	20021027	44.4	-170.9	-127	Fig. 3b
20021002	20021026	23.8	-164.4	-69	Fig. 3c

Modeling — Preliminary Results

The earthquakes were modeled as rectangular dislocations in an elastic half space, following the formulations of *Okada* [1985]. The 3-D displacements predicted by the dislocation models were converted into line-of-sight displacements by projecting along the satellite look direction calculated at each observation location, and solutions were sought that minimized the squared misfit between the calculated and observed phase changes.

Nenana Mountain earthquake. For the 23 October earthquake, the fault geometry and magnitude of slip for the single fault plane was determined to be the best fit to interferograms (Figure 3a-3c). The best-fit fault plane is 21 km long, and has a strike, dip, and rake of 263°, 86°, and 175°, respectively. There is a strong tradeoff between the magnitude of slip on the fault plane and the depth extent of faulting—solutions with narrow fault planes centered at a depth of 10 km and high slip, and have the same misfit and moment as solutions with less slip on wider faults. If slip is fixed at 2 m, the depth range of faulting inferred is 7.3 to 14.6 km; a slip of 1 m results in a depth range of 5.3 to 23.0 km. A synthetic interferogram calculated using the same imaging geometry as that used for Figures 3a-3b (Figure 3d) shows our model fit to the interferograms (Figures 3a-3c) very well [see *Wright et al.*, 2003].

Denali Fault earthquake. Because of the size and complexity of the large earthquake on the Denali Fault, more than one fault plane was necessary to model the InSAR data (Figures 1, 2a-2b). However, near-fault incoherence in the data restricts its ability to resolve the details of slip on the fault plane. Due to lack of coherent interferograms, only the western half of the earthquake rupture was modeled. The model therefore consists of just three fault patches—one beneath the Susitna Glacier Fault and two along the main Denali Fault.

For the Susitna Glacier Fault segment, interferograms (Figures 1 and 2a) contain coherent data close to the fault rupture, and hence the best fit fault geometry, location and slip were solved. The best-fit uniform slip model has 7 m of slip on the Susitna Glacier Fault at depth, between 1.0 and 10.1 km. The model fault plane is 30 km long; has a strike, dip, and rake of 251°, 40°, and 88° respectively; and has a moment magnitude of 7.2.

Farther to the east, the fault location is poorly determined by the InSAR data. The surface rupture location was fixed to that of the mapped fault trace, and it is assumed that the fault is vertical with pure right-lateral slip. Slip on two segments were solved. The first of these is 55 km long and extends from the western end of the strike-slip rupture on the Denali Fault to the location where the strike of the fault

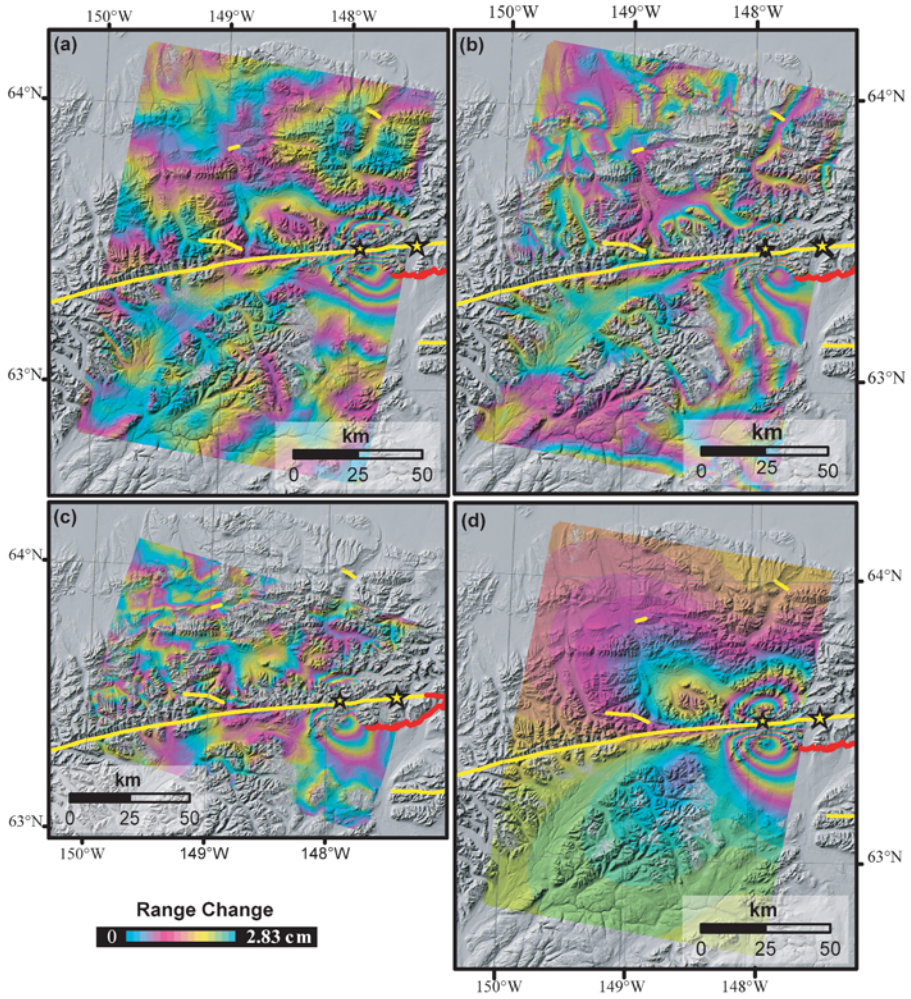

Fig. 3. (a-c) Radarsat-1 interferograms showing ground surface deformation associated with the 23 October Nenana earthquake. Image acquisition times are shown in Table 1. (d) A synthetic interferogram using parameters that best fit the observed interferograms.

changes, ~12 km west of the pipeline crossing. The second segment, 155 km long, extends from this point to the junction with the Toschunda Fault in the east. Slip on the Toschunda Fault was not included in the model because there is no coherent InSAR data at present within 150 km of this fault. Because large surface ruptures were observed, it is assumed that the slip reached the surface and we hence solve for just three parameters—slip on the two large patches, and a single depth extent applied to both patches. The best-fit slip on the western, strike-slip fault segment was 4.1 m, with 7.2 m of slip on the eastern segment, extending from the surface to a depth of 12.2 km. The synthetic interferogram, calculated using this model and the same imaging geometry as that used for Figure 1, is shown in Figure 2d.

Discussions, Conclusions

Based on the model (Figure 3d), the moment magnitude for the 23 October Nenana earthquake is M_w 6.7. This is consistent with estimates from seismology (Harvard CMT M_w = 6.6; USGS CMT M_w = 6.7; Alaskan Earthquake Information Center (AEIC) M_w = 6.7). The modeled strike/dip/rake of 263°/86°/175° are very similar to those obtained by modeling the teleseismic body waveform (265°/80°/179°) [*Kikuchi and Yamanaka*, 2002], and by first motion focal mechanism data from AEIC (263°/90°/175°). The model predicts that any slip observed at the surface for this earthquake will be negligible, when compared to the slip occurring on the fault plane at depth.

The model for the Susitna Glacier Fault suggests that thrusting associated with the 3 November 2002 rupture has a strike/dip/rake of 251°/40°/88°, respectively. This implies almost pure thrust motion at depth, in approximate agreement with the first motion analysis carried out by the AEIC (262°/48°/115°) and waveform inversion by *Kikuchi and Yamanaka* [2002] (227°/40°/99°). The strike of the fault plane obtained from InSAR data (i.e., 251°) is similar to that from first motion data (i.e., 262°), but both are larger than that derived from teleseismic waveform inversion (i.e., 227°). The dip of the fault plan is about 40° from our model, about 48° from the AEIC first motion data, and about 35–40° from the seismic waveform inversion [*Ji et al.*, 2002; *Kikuchi and Yamanaka*, 2002]. These values are twice as much as the surface dip from the field data, suggesting the dip decreases as the fault approaches the surface [*Eberhart-Phillips et al.*, 2003].

C-band radar coherence is lost within 5–10 km of the Denali Fault in 24 days, which made it impossible to map the detailed deformation near the rupture zone. To improve the coherence, future InSAR missions should be equipped with radar of longer wavelength, and allow shorter repeat intervals (a few days) to improve interferometric coherence over glaciated areas.

Acknowledgments

Radarsat-1 SAR images are copyright© 2002 Canadian Space Agency, and provided by the Alaska SAR Facility (ASF). This research was supported by funding from NASA, USGS contract O3CRCN0001, USGS Geography Discipline Prospectus Fund, USGS Earthquake Hazards Program, and NERC Research Fellowship. We thank ASF staff members for their world-class service in providing the SAR data; P. Haeussler, G. Fuis, and M.L. Zoback for various assistance; T. Masterlark and W. Thatcher for technical reviews; and *Eos* editor J. Geissman and a reviewer for comments and suggestions.

References

Eberhart-Phillips, D., et al., The 2002 Denali fault earthquake, Alaska: a large magnitude, slip-partitioned event, *Science, 300*, 1113–1118, 2003.

Ford, A., R. Bruhn, and R. Forster, InSAR measurements of surface deformation in the epicentral region of the Nenana Mountain and Denali fault earthquakes of Oct. 27 and Nov. 3, 2002 (abstract), *Eos Trans. AGU, S72F*, 1369, 2002.

Ji, C., D. Helmberger, and D. Wald, Preliminary slip history of the 2002 Denali earthquake (abstract), *Eos Trans. AGU, S72F*, 1344, 2002.

Kikuchi, M., and Y. Yamanaka, Source rupture processes of the central Alaska earthquake of Nov. 3, 2002, inferred from teleseismic body waves, EIC Seismological Note, No. 129, Nov. 4, 2002.

Massonnet, D. and K. Feigl, Radar interferometry and its application to changes in the Earth's surface, *Rev. Geophys., 36*, 441–500, 1998.

Okada, Y., Surface deformation due to shear and tensile faults in a half-space, *Bull. Seismol. Soc. Am. 75(4)*, 1135–1154, 1985.

Wright, T. J., Z. Lu, C. Wicks, and W. Thatcher, Coseismic deformation of the 2002 Denali fault (Alaska) earthquakes from InSAR: preliminary results and prospects (abstract), *Eos Trans. AGU, S72F*, 1370, 2002.

Wright, T.J., Z. Lu, and C. Wicks, Source model for the Mw 6.7, 23 October 2002, Nenana Mountain Earthquake (Alaska) from InSAR, *Geophys. Lett., 30,* 18, 1974, doi: 10.1029/2003GL018014, 2003.

Author Information

Zhong Lu, SAIC, EROS Data Center, U.S. Geological Survey, Sioux Falls, S.D.; Tim Wright, COMET, Oxford University, U.K.; Chuck Wicks, Earthquake Hazards Program, USGS, Menlo Park, Calif.